NASA TECHNICAL NOTE

NASA TN D-4738

$c. 1$

INVESTIGATION OF ELECTRON-RADIATION-INDUCED DIELECTRIC BREAKDOWNS IN A TYPICAL CAPACITOR METEOROID DETECTOR SYSTEM

by George M. Storti, George E. Rambo, Herbert D. Hendricks, and Thomas B. Ballard

Langley Research Center
Langley Station, Hampton, Va.

NATIONAL AERONAUTICS AND SPACE ADMINISTRATION • WASHINGTON, D. C. • SEPTEMBER 1968

NASA TN D-4738

INVESTIGATION OF ELECTRON-RADIATION-INDUCED DIELECTRIC

BREAKDOWNS IN A TYPICAL CAPACITOR METEOROID

DETECTOR SYSTEM

By George M. Storti, George E. Rambo, Herbert D. Hendricks,
and Thomas B. Ballard

Langley Research Center
Langley Station, Hampton, Va.

NATIONAL AERONAUTICS AND SPACE ADMINISTRATION

INVESTIGATION OF ELECTRON-RADIATION-INDUCED DIELECTRIC

BREAKDOWNS IN A TYPICAL CAPACITOR METEOROID

DETECTOR SYSTEM

By George M. Storti, George E. Rambo, Herbert D. Hendricks,
and Thomas B. Ballard
Langley Research Center

SUMMARY

The effects of electron radiation on capacitor-type detector systems similar to those used on the Pegasus satellite were investigated. Each system that was tested consisted of a polyurethane foam panel containing two capacitor-type-meteoroid detectors, several meters of polyethylene terephthalate insulated electrical leads, and other items such as rubber shock mounts and polyethylene terephthalate adhesive tape. Three different target thicknesses for the meteoroid detectors were tested, these thicknesses being 40, 200, and 400 microns (1.5, 8, and 16 mils).

The incident kinetic energy of electrons used in the tests ranged from 30 keV to 1000 keV, and the temperature of the detector systems was maintained at either 197° K or 297° K. It was found that radiation-induced dielectric breakdowns were produced in the systems and that some of these signals were indicated as meteoroid penetrations. It was determined that the primary source of the breakdowns and, hence, the penetration indications was the polyethylene terephthalate insulated wire. The number of breakdowns and penetration indications obtained for a fluence of 5×10^{13} e/cm^2 was found to be dependent on the incident kinetic energy of the electrons and the system temperature; that is, more breakdowns and penetration indications occurred at the lower temperature (197° K) and the lower energies (30 keV to 100 keV). Tests were performed with different modifications made to the signal processing circuits. Several of these modifications resulted in a significant reduction or the total elimination of the radiation-induced penetration indications. Finally, it was found that those systems containing 200 and 400 micron detectors with 200- and 400-micron-thick targets suffered severe decreases in resistance in the capacitor-type detectors.

INTRODUCTION

Several types of meteoroid detectors have been developed to provide a direct measurement of the frequency of meteoroid penetrations as a function of known thickness of

known materials. Among these detectors is the capacitor-type which was developed at the Langley Research Center. This type detector was found to exhibit excellent detection characteristics in early testing, and the associated detector electronic circuits were relatively simple and easily constructed. Because of these and other advantages, the capacitor detector was chosen as the type detector to be included on the Pegasus series of meteoroid detection satellites (refs. 1 and 2).

As part of the development program, both detectors and associated hardware were subjected to a variety of tests. Among the tests was an attempt to determine the effects of electron irradiation on complete detector systems. (In addition to the detectors themselves, the systems included the support panels for the detectors, polyethylene terephthalate ribbon wire and tape, and rubber shock mounts.) The radiation tests were prompted by the fact that (1) the satellites containing the exposed detector systems would be passing through part of the earth's radiation belts (refs. 3 and 4) and (2) previous tests indicated that charge storage with subsequent dielectric breakdown took place in dielectric materials when exposed to electron irradiation (ref. 5). These breakdown signals reported in reference 5 had a shape that was similar to the signals expected to be produced by meteoroid penetrations. Hence, the signals might be indistinguishable to the signal processing and recording circuits. Consequently, the objectives of the irradiation tests were (1) to determine the sources of the breakdowns in the detector systems, (2) to determine the magnitude of the occurrence of the breakdowns, and (3) to minimize the effect of the breakdowns by making changes in the detector electronics.

Extensive tests were carried out on detector systems containing detectors having a target thickness of 40 microns. (These detectors are hereinafter referred to as 40 micron detectors.) Other tests were made in which the detector systems contained detectors having 200- and 400-micron-thick targets. (These detectors are hereinafter referred to as 200 micron and 400 micron detectors.) The number of breakdowns and the number of penetration indications produced by the breakdowns in the detector electronics were monitored for a given fluence of electrons. Filter circuits were designed to discriminate against the penetration indications produced by the radiation-induced breakdowns.

APPARATUS AND TESTS

Accelerator

The detector systems were irradiated with a beam of monoenergetic electrons produced by a cascaded-rectifier potential drop accelerator (ref. 6). This accelerator furnished direct-current beams of electrons having incident kinetic energies ranging from 30 keV to 1000 keV.

The accelerator energy was calibrated by using a solid-state radiation detector which, in turn, was calibrated with suitable radioactive isotopes. The energy spread of the beam and the short-term energy fluctuations were less than the 18-keV (full width at half maximum) resolution of the detector. However, the actual energy of the beam was believed to be within 1.0 percent of the nominal value stated.

Target Chamber

The target chamber used for these tests was cylindrical with a diameter of 2.13 meters and a length of 4.88 meters (fig. 1). The chamber and the beam-handling system were evacuated to a pressure of 2.67×10^{-4} N/m^2 $\left(2 \times 10^{-6} \text{ torr}\right)$ by using six large oil-diffusion pumps. The interior of the target chamber was equipped with cryogenic panels to cool the test samples. Targets were mounted at the end of the chamber in an aluminum frame. The aluminum frame was supported on knife edges so that the detector systems were cooled by thermal radiation. The temperature of the target system was monitored by a thermocouple mounted on the aluminum frame.

Beam Characteristics

Electrons produced by the accelerator passed through an evacuated beam tube into beam-handling and target-chamber systems (fig. 1). By the use of steering, focusing, and spreading magnets, the beam was directed into the target chamber. The beam was spread by a quadrupole magnet just prior to entering a chamber containing a collimator. The collimator limited the cross-sectional area of the beam entering the target chamber so as to prevent the scattering of electrons off the target-chamber walls. The diverging beam traversed the length of the chamber and impinged upon the target (fig. 1). An area of at least 0.62 m by 1.11 m was bombarded by the beam. This area included the entire detector system when mounted in the aluminum supporting frame. The beam current uniformity over this area was determined by swinging Faraday cups over the target about axes located directly above and directly to the right of the target (fig. 2). (The outline of the target area is seen in the pattern on the aluminum plate.) The midway position in the arc swept by each Faraday cup was the same. The density of the spread beam was found to be uniform in these arcs to within ±15 percent of the stated current densities $\left(\text{expressed in e/cm}^2\text{-sec}\right)$. In addition, a secondary check on the beam current uniformity was made by simply observing (with the aid of closed-circuit television) the fluorescence of zinc sulfide that was applied to an aluminum plate at the target area.

The beam current density during tests was monitored by a biased Faraday cup (200 volts negative). Figure 3 shows the position of the Faraday cup relative to the target. Current collected by the Faraday cup was fed through an integrating electrometer (accuracy within 2 percent of indicated values) to the ground to measure the flux in e/cm^2-sec and the total fluence in e/cm^2.

Test Samples

The complete detector system consisted of the meteoroid detector panel, rubber shock mounts, polyethylene terephthalate insulated ribbon wire, and polyethylene terephthalate adhesive tape (figs. 3 to 5). The detector panels consisted of two 50- by 100-cm parallel-plate capacitors separated by a 2.5-cm layer of polyurethane foam (fig. 5). The capacitor-type detectors were formed by backing either 40-, 200-, or 400-micron-thick aluminum target plates with a 12-micron-thick polyethylene terephthalate trilaminate which, in turn, was backed by a 0.07-micron-thick layer of vapor-deposited copper. Type 1100-0 aluminum was used for the 40 micron detectors and 2024T-3 aluminum was used for the 200 and 400 micron detectors. An Alodine thermal control coating was placed on the outer aluminum surface of the detectors (ref. 2).

Mounted on the detector panel were two terminal blocks to which electrical connections could be made to the two detectors (fig. 4). A resistor-diode network was placed in each terminal block. Much of the terminal block was encased with dielectric material in order to provide electrical insulation between the two detector terminals. Dielectric material was also present at the six points at which the detector panel was attached to the supporting frame. Rubber shock mounts were used at these positions for this attachment purpose (fig. 3).

Polyethylene terephthalate insulated ribbon wire was used to connect the detectors to the readout electronics. Approximately 16 meters of this ribbon wire was attached (with the polyethylene terephthalate tape) to the aluminum supporting frame. (This was done since wire segments of several meters in length are required on large meteoroid detection satellites such as Pegasus.) This wire consisted of eight flat copper wires (0.07 mm thick) imbedded in 0.02 millimeter of polyethylene terephthalate. Four of the wires were used to connect to the detectors and the other four were grounded.

Test Circuits

The basic readout circuitry as used in the experiment is seen in figures 6 and 7 and was designed to operate in the following manner. When a meteoroid passes through the capacitor-type detector (charged to 44 volts), a plasma is created momentarily in the region of penetration. Conduction through the plasma causes a temporary discharge of the biased detector. After the plasma dissipates, conduction ceases and the detector recharges at a rate characteristic of the capacitance and resistance of the recharge circuit. The resultant signal produced by the penetration passes through a resistor-diode isolation network and the polyethylene terephthalate insulated ribbon wire to the detector electronics. The input signal from the detector system passes through an input filter of the detector electronics which is designed to suppress any high-frequency radiation-induced signals. Next, it passes through a coupling capacitor, a diode, and another

4

filtering circuit to an integrating amplifier. Simultaneously, the signal starts a one-shot multivibrator which, in essence, acts as a timer for the integrating amplifier. The integrator functions for 250 microseconds and the resultant signal from the integrating amplifier is fed to a Schmitt trigger. If the voltage time product of the breakdown signal is greater than a given value, the Schmitt trigger produces a signal having an amplitude of 4 volts and a duration of 5 milliseconds which is transmitted to monitoring and recording circuits (fig. 7). In the tests reported herein, the discrimination level for the Schmitt trigger was usually set such that a transient having an amplitude greater than 2.9 volts and a decay corresponding to the RC time constant of the detection electronics would be recorded as a penetration indication. (Trigger levels different from 2.9 volts are specifically noted in the pertinent places.) This discrimination level was maintained within ±0.2 volt of the nominal voltage setting.

The breakdown signal and the resulting signals produced in the detector electronics were monitored with the instrumentation seen in figure 7. Specifically, the breakdown signal was monitored by oscilloscope 1 and the integrator output and penetration indications were monitored by oscilloscope 2. The trigger level in oscilloscope 1 was usually set such that only breakdowns having an amplitude greater than 28 volts would be accepted. Gating signals produced in oscilloscope 1 by such breakdowns were used to trigger oscilloscope 2 so that the breakdown, integrator output, and penetration indication signals could be displayed simultaneously. The number of breakdowns were recorded on counters that accepted a gating signal from oscilloscope 2. Penetration indications were recorded by passing the output of the detector electronics directly to counters. Both detectors of the detector systems were monitored in this manner. Photographs were obtained of the oscilloscope traces produced by the breakdown, the integrator output, and the penetration indication signals.

A minor circuit change was made to the detector systems during the tests. This change involved the replacing of a 1000-ohm resistor on the terminal board of the detectors with a 1-megohm resistor. This change had negligible effect on the data.

Test Program Outline

The outline of the test program on the meteoroid detector systems is as follows. For each part of the program the systems tested, the purpose of the tests, and the test conditions are given.

I. Tests on detector system 1, 40 micron detectors (original input filter, fig. 6, was used):

Purpose: Determination of the sources of radiation-induced breakdowns in the detector system

Test conditions: System temperature, 197° K; kinetic-energy range, 30 keV to 250 keV; electron flux, 10^{10} e/cm^2-sec

Note: The resistance R was 1000 ohms

II. Tests on detector system 2, 40 micron detectors (original input filter, fig. 6, was used):

Purpose: Determination of the effect of kinetic energy and temperature on the radiation-induced breakdowns and penetration indications

Test conditions: System temperature, 197° K or 297° K; kinetic-energy range, 30 keV to 250 keV; electron flux, 10^{10} e/cm^2-sec; inputs to detector electronics from detectors, normal or reversed

Note: The resistance R was 1000 ohms

III. Tests on detector system 3, 40 micron detectors:

A. Purpose: Determination of the effects of intermittent irradiation on the production of breakdowns and penetration indications (original input filter, fig. 6, was used)

B. Purpose: Reduction of the effects of breakdowns in the detector electronics by making input filter modifications (the ribbon wire used in all previous tests was replaced by an unirradiated segment during this section of the test program)

Test conditions: System temperature, 197° K; kinetic-energy range, 30 keV to 250 keV; electron flux, 10^{10} e/cm2-sec

Note: The resistance R was 1 meghom

IV. Tests on detector systems containing 200 and 400 micron detectors (original input filter, fig. 6, was used)

Purpose: Determination of the effect of kinetic energy on the production of breakdowns and penetration indications

Test conditions: System temperature, 197° K; kinetic-energy range, 300 keV to 1000 keV; electron flux 10^{10} e/cm^2-sec

Note: The resistance R was 1 meghom

RESULTS AND DISCUSSION

The detector systems were tested under severe environmental conditions; that is, the systems were irradiated by using a flux $\left(10^{10} \text{ e/cm}^2\text{-sec at all energies}\right)$ higher than might be encountered by the Pegasus satellites, and the temperature (197° K $\pm$ 40° K) at which the greatest number of tests were conducted was lower than that to be expected. In addition, the laboratory irradiations were for the most part carried out by using a steady electron flux whereas the Pegasus satellites would experience significant fluxes of electron radiation only when it entered the South Atlantic anomaly of the radiation belts. This serves to point up the great difficulty in simulating the space environment.

Detector System 1

The first detector system tested was one with 40 micron detectors (part I of test program outline). However, only one of the detectors was operative; the other detector (the detector not exposed directly to the beam) was found to be short circuited. Consequently, only the operable detector with its associated circuitry was involved in the testing. Both the number of breakdowns and the number of penetration indications were monitored.

First, the entire detector system was irradiated. Next, the detector panel containing the detectors, the ribbon wire, and the tape were irradiated with the rubber shock mounts being replaced by metal screws. In the final case, only the detector panel containing the detectors was irradiated. The ribbon wire was replaced by uninsulated copper wire and the shock mounts by metal screws. The results on detector system 1 are seen in table I.

With the entire system being irradiated, a considerable number of penetration indications were obtained. When the ribbon wire, tape, and detector panel were tested, a great many breakdowns and penetration indications were still obtained. However, when only the detector panel was irradiated (all other insulated components replaced), very few penetration indications and relatively few breakdowns were obtained (even though the trigger level for the acceptance of the breakdowns was reduced). These results indicated that the major source of breakdowns and penetration indications was the polyethylene terephthalate insulated ribbon wire and tape. The presence of Lichtenberg figures (permanently visible patterns caused by the discharges) in the ribbon wire supported this conclusion. Additional evidence obtained from the examination of the photographs of the breakdown signals indicated that the breakdowns originated in the ribbon wire. The decay time constant of the breakdowns seen in the photographs (2 to 5 microseconds) was considerably less than that expected from breakdowns originating in the

detector (approximately 3 milliseconds). This difference is attributable to the large difference in capacitance in the ribbon wire and the detector.

Detector System 2

Tests were made on a second detector system with 40 micron detectors in order to determine the effects of incident kinetic energy (30 to 250 keV) and temperature (197° K and 297° K) on the number of breakdowns and penetration indications (part II of the test program outline). Figures 8 to 11 show the results of these tests on detector system 2. Included in these figures are results obtained when the two inputs to the electronics (channels 1 and 2) from the two detectors were interchanged. This interchanging was done in order to assure the fact that each channel of the detector electronics performed its function in a similar manner.

Some general features can be observed in all these results. The greatest number of breakdowns and penetration indications were obtained at the lower energies with a subsequent decrease at the higher energies. This result is due to the fact that more electrons are stopped and trapped in the materials at the lower energies than at the higher energies. Consequently, less fluence is required to cause breakdown in the material. This condition is in substantial agreement with trends observed in capacitors and insulated wires as reported in reference 5. Also in agreement with reference 5 is the effect of temperature on the production of breakdowns. Considerably fewer breakdowns and penetration indications were obtained at 297° K than at 197° K. However, the evidence is inconclusive as to whether the switching of inputs had any effect on the results; that is, essentially the same results were obtained from the front (or rear) detector regardless of whether the inputs to the detector electronics were switched.

Photographs of two breakdown signals along with the associated integrator output and penetration indication signals are seen in figures 12 and 13. The breakdowns are characterized by a very fast rise time which is on the order of a few nanoseconds and a subsequent decay corresponding to the RC time constant of the ribbon wire and detection circuit (not including the meteoroid detector). At the forward edge of the signal, high amplitude ringing is observable (fig. 12). This ringing is believed to be due to inductances in the test system. In figure 13, two types of penetration indication signals are observable. The pulse shape seen in the top photograph of figure 13 was that expected from the electronics when the detector electronics processed the penetration signal as designed. However, the majority of penetration indication pulse shapes were similar to that seen in the bottom photograph of figure 13. The pulse shapes indicate that the detector electronics were not processing the signal correctly; that is, the signal was bypassing the integrating circuit and directly triggering the Schmitt trigger. (It may be recalled that when the electronics operate as designed the integrator output signal triggers the Schmitt trigger when the time-voltage product is greater than a given threshold value.)

8

Detector System 3

Some tests were conducted on a third detector system with 40 micron detectors in order to determine the effects of intermittent electron irradiation (part IIIA of the test program outline). This was done in order to approximate more closely the expected orbital environment. The detector system was irradiated for only a period of 50 seconds in a 300-second period. The beam was switched off and on in this manner until the system had received a fluence of 5×10^{13} e/cm^2. Results of the number of breakdowns and penetration indications obtained for this dose on detector system 3 are seen in table II(a). In addition to the fact that breakdowns and penetration indications occurred during the irradiation period, it was found that a few of each occurred during the period when there was no irradiation. (By far the greatest number, however, occurred during irradiation.)

As a consequence of the generally unsatisfactory operation of the detector electronics, it became obvious that circuit modifications were necessary to reduce the effects of the irradiation. Hence, new input filters to the detector electronics were designed and tested (part IIIB of the test outline program). The results of these tests are seen in tables II(b) to II(h). It was found that filters 3, 4, and 5 were the most effective in reducing the effects of the breakdowns in the detector electronics. Few penetration indications resulted even though many breakdowns occurred in the detector system. It was also found that filter 6 considerably reduced the effects of the breakdowns. In addition, filter 6 caused the signals to be processed in the detector electronics as designed. Consequently, several filter configurations were found that reduced the probability that radiation-induced breakdowns would cause penetration indications.

Detector Systems Containing 200 and 400 Micron Detectors

Five 200 micron and two 400 micron detector systems were irradiated in order to determine the effects of higher energy electrons (300 to 1000 keV) on the production of penetration indications. (See part IV of test program outline.) These results are seen in table III. It was found that considerably fewer breakdowns and very few penetration indications occurred even though the original input filter was used in the detector electronics. In addition, it was found that the resistance of at least one of the two detectors contained in each detector system decreased from approximately 2×10^9 ohms to less than 5×10^6 ohms after having received a fluence of 1.5×10^{14} e/cm^2. In most cases, this marked decrease in resistance occurred in the detector that was being bombarded directly by the electron beam. It was also noted that these resistance decreases occurred after the detectors had been bombarded with 500- to 1000-keV electrons. The causes of this behavior have not been determined.

However, before the detectors had developed the severe resistance decreases, some photographs of the breakdowns and penetration indications were obtained. It was found that some of the breakdown signals had decay times indicating their origin to be the 12-micron-thick polyethylene terephthalate of the meteoroid detector; that is, the signals had decay time constants corresponding to the resistance of the detector electronics and the capacitance of the meteoroid detector. Hence, radiation-induced breakdowns were obtained in the detectors in addition to the other insulating materials used in the detector systems.

CONCLUSIONS

The effects of electron radiation in combination with temperature and vacuum on capacitor-type meteoroid detector systems, similar to those used on the Pegasus satellite, were investigated. Variable parameters studied were electron kinetic energy (30 to 1000 keV) and temperature (197° K or 297° K). Dielectric breakdowns were detected and subsequently studied to determine the source. Electronic filter circuits were designed to eliminate or reduce the effects of dielectric breakdowns on the electronic detector system. The following conclusions were reached from this study:

1. Dielectric breakdowns caused by the electron irradiation produced penetration indications in the meteoroid detector systems tested. Filter networks were designed that considerably reduced the effects of the breakdowns in the detector electronics and, in some cases, completely eliminated them.

2. Breakdowns were produced primarily in the polyethylene terephthalate ribbon wire of the detector systems although there were other sources such as the polyethylene terephthalate dielectric of the meteoroid detectors.

3. The number of breakdowns and penetration indications obtained for a given fluence was dependent on the temperature and incident electron kinetic energy. Fewer breakdowns were obtained at 297° K than at 197° K. Also, fewer breakdowns were obtained at the higher kinetic energies (100 to 1000 keV) than at the lower kinetic energies (30 to 100 keV).

4. Tests on 200 and 400 micron detector systems at 197° K with incident energies between 500 and 1000 keV showed that both types of detectors were susceptible to the development of permanent decreases in resistance. The resistance decrease occurred before the detector systems had been exposed to a fluence of 1.5×10^{14} e/cm2.

Langley Research Center,
National Aeronautics and Space Administration,
Langley Station, Hampton, Va., March 5, 1968,
124-09-12-05-23.

REFERENCES

1. Naumann, Robert J.: Pegasus Satellite Measurements of Meteoroid Penetration (Feb. 16-July 20, 1965). NASA TM X-1192, 1965.

2. Anon.: The Meteoroid Satellite Project Pegasus First Summary Report. NASA TN D-3505, 1966.

3. Hess, W. N., ed.: Collected Papers on the Artificial Radiation Belt From the July 9, 1962, Nuclear Detonation. J. Geophys. Res., vol. 68, no. 3, Feb. 1, 1963, pp. 605-758.

4. Vette, James I.: Models of the Trapped Radiation Environment. Volume I: Inner Zone Protons and Electrons. NASA SP-3024, 1966.

5. Storti, George M.; Phillips, Donald H.; and Frank, Clifford S.: Experimental Study of Transient Effects in Dielectric Materials Caused by Electron Irradiation. NASA TN D-3032, 1965.

6. Cleland, M. R.; and Morganstern, K. H.: A New High-Power Electron Accelerator. IRE, Trans. Ind. Electron., vol. IE-7, no. 2, July 1960, pp. 36-40.

TABLE I.- RESULTS OF ELECTRON IRRADIATION TESTS ON DETECTOR SYSTEM 1

FOR THE PURPOSE OF DETERMINING THE SOURCE OF RADIATION-INDUCED

BREAKDOWNS AND PENETRATION INDICATIONS

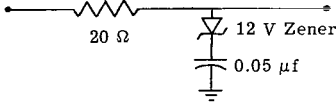| Incident electron kinetic energy, keV	Total electron fluence, e/cm^2	Number of voltage breakdowns obtained	Number of penetration indications obtained
Radiation tests with entire detector system exposed to beam			
50	10^{14}	882 ⎫	43
50	7.5×10^{13}	760 ⎬ $\geqq$ 28 V	32
250	1.26×10^{14}	139 ⎭	0
50	5.1×10^{13}	2430 ⎫ $\geqq$ 5 V	52
75	1.26×10^{14}	4116 ⎭	30
Radiation tests with detectors, ribbon wire, and adhesive tape exposed to beam			
30	5×10^{13}	178 ⎫	19
50		320	14
75		926	44
75		880 ⎬ $\geqq$ 28 V	45
100		243	5
150		113	0
200		193	3
250		324 ⎭	3
Radiation tests with only detectors exposed to beam			
30	1.73×10^{13}	0 ⎫	0
50	5×10^{13}	93	0
75		140	0
100		94 ⎬ $\geqq$ 10.3 V	5
150		113	0
200		114	0
250		41 ⎭	0

TABLE II.- RESULTS OBTAINED FROM DETECTOR SYSTEM 3
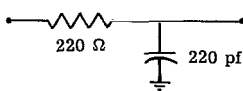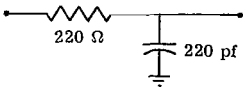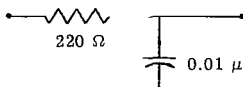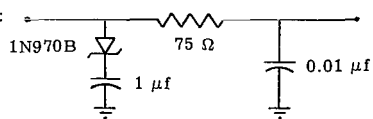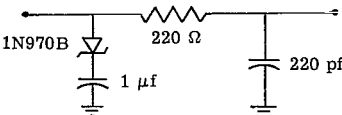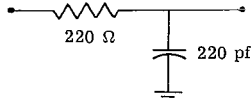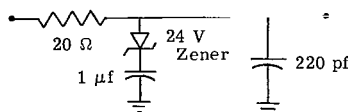
Incident electron kinetic energy, keV	Number of voltage breakdowns obtained for fluence of 5×10^{13} e/cm^2		Number of penetration indications obtained for fluence of 5×10^{13} e/cm^2	
	Front detector	Rear detector	Front detector	Rear detector

(a) Intermittent radiation tests (beam on 50 sec, off 250 sec until fluence of 5×10^{13} e/cm^2 was obtained)

Input filter: 220 Ω — 220 pf

	Front detector	Rear detector	Front detector	Rear detector
75	387 } ≧ 28 V	538 } ≧ 28 V	22	25
75	627	776	26	23

(b) Radiation tests on detector system 3 using original input filter 1

Input filter: 220 Ω — 220 pf

	Front detector	Rear detector	Front detector	Rear detector
30	148	143	9	3
50	458	527	22	8
75	530	620	28	21
100	269 ⟩ ≧ 28 V	238 ⟩ ≧ 28 V	22	11
150	99	192	8	5
200	162	275	3	5
250	28	97	0	3

(c) Radiation tests on detector system 3 using input filter 2

Input filter: 220 Ω — 0.01 μf

	Front detector	Rear detector	Front detector	Rear detector
30	87	84	0	1
50	325	238	2	3
75	387	407	7	8
100	236 ⟩ ≧ 28 V	268 ⟩ ≧ 28 V	19	6
150	81	173	3	7
200	87	190	4	8
250	91	249	0	6

(d) Radiation tests using input filter 3

Input filter: 1N970B — 75 Ω — 1 μf — 0.01 μf

	Front detector	Rear detector	Front detector	Rear detector
30	170	Not monitored	0	0
50	382		0	0
75	905 ⟩ ≧ 28 V		0	1
100	194		1	0
150	73		0	0
200	17 } ≧ 10 V		0	0
250	10		0	0

13

TABLE II.- RESULTS OBTAINED FROM DETECTOR SYSTEM 3 — Concluded

Incident electron kinetic energy, keV	Number of voltage breakdowns obtained for fluence of 5×10^{13} e/cm²		Number of penetration indications obtained for fluence of 5×10^{13} e/cm²	
	Front detector	Rear detector	Front detector	Rear detector

(e) Radiation tests using input filter 4

Input filter: 1N970B — 220 Ω — 1 μf — 220 pf

Incident electron kinetic energy, keV	Front detector (breakdowns)	Rear detector (breakdowns)	Front detector (penetration)	Rear detector (penetration)
30	153 ⎫	Not monitored	0	1
50	757 ⎪		0	0
75	655 ⎪		0	0
100	538 ⎬ ≧ 10 V		0	0
150	402 ⎪		0	0
200	489 ⎪		0	0
250	291 ⎭		0	0

(f) Radiation tests using original input filter[a]

Input filter: 220 Ω — 220 pf

Incident electron kinetic energy, keV	Front detector (breakdowns)	Rear detector (breakdowns)	Front detector (penetration)	Rear detector (penetration)
50	450 ⎫	570 ⎫	213	93
75	294 ⎬ ≧ 28 V	200 ⎬ ≧ 28 V	54	18
100	1066 ⎭	566 ⎭	69	13

(g) Radiation tests using input filter 5 [a]

Input filter: 20 Ω — 1 μf — 24 V Zener — 220 pf

Incident electron kinetic energy, keV	Front detector (breakdowns)	Rear detector (breakdowns)	Front detector (penetration)	Rear detector (penetration)
50	773 ⎫	577 ⎫	0	0
75	365 ⎬ ≧ 20 V	244 ⎬ ≧ 20 V	0	0
100	1443 ⎭	801 ⎭	0	0

(h) Radiation tests using input filter 6 [a]

Input filter: 20 Ω — 12 V Zener — 0.05 μf

Incident electron kinetic energy, keV	Front detector (breakdowns)	Rear detector (breakdowns)	Front detector (penetration)	Rear detector (penetration)
50	625 ⎫	521 ⎫	14	0
75	913 ⎬ ≧ 10 V	697 ⎬ ≧ 10 V	20	0

[a]Ribbon wire used in all previous tests replaced by a new segment.

TABLE III.- RESULTS OF TESTS ON 200 AND 400 MICRON DETECTOR SYSTEMS

[The input filter used in the detection circuit was the original filter (220 Ω, 220 pf)]

Detector system	Type	Kinetic energy, keV	Number of breakdowns ≧ 28 volts		Number of penetration indications		Resistance at failure		Fluence, e/cm²	Comments
			Front	Rear	Front	Rear	Front	Rear		
4	200μ	400	5	31	0	0	------	------	5×10^{13}	Penetration indication trigger level = 5 volts
		800	0	4	0	0	405 KΩ	>10^9 Ω	5×10^{13}	
5	200μ	300	60	233	0	3	------	------	5×10^{13}	
		900	0	0	0	0	------	------	5×10^{13}	
		500	13	22	0	0	280 KΩ	240 KΩ	5×10^{13}	
6	200μ	600	2	0	1	0	500 KΩ	>10^9 Ω	5×10^{13}	
7	200μ	700	308	0	0	0	------	------	5×10^{13}	
		1000	0	0	0	0	11 KΩ	>10^9 Ω	5×10^{12}	
8	200μ	500	0	1	0	0	------	------	5×10^{13}	
		600	5	3	0	0	170 KΩ	>10^9 Ω	5×10^{13}	
9	400μ	300	68	184	1	9	------	------	5×10^{13}	Penetration indication trigger level = 2.9 volts
		400	2	24	1	0	------	------	5×10^{13}	
		500	2	20	0	0	50 MΩ	2.7 MΩ	5×10^{13}	
10	400μ	600	0	0	0	0	------	------	5×10^{13}	
		700	10	3	44	0	1.3 KΩ	>10^9 Ω	1×10^{14}	
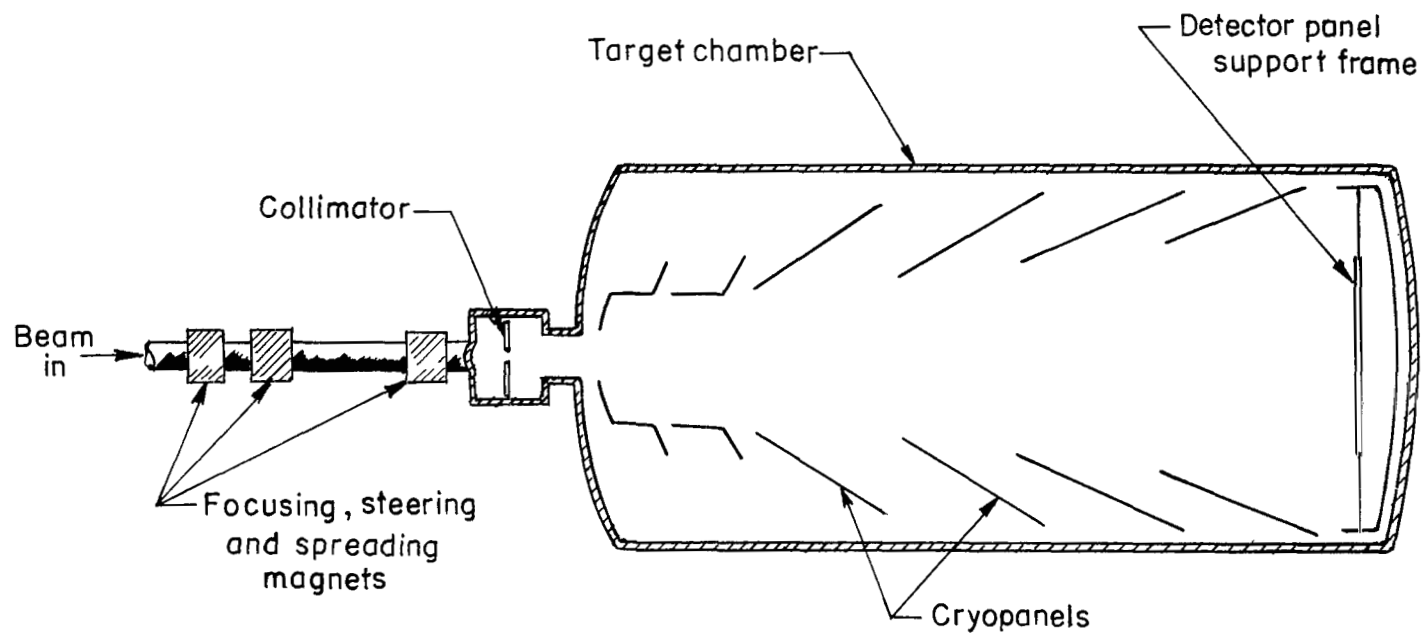
Figure 1.- Beam handling and target chamber systems.
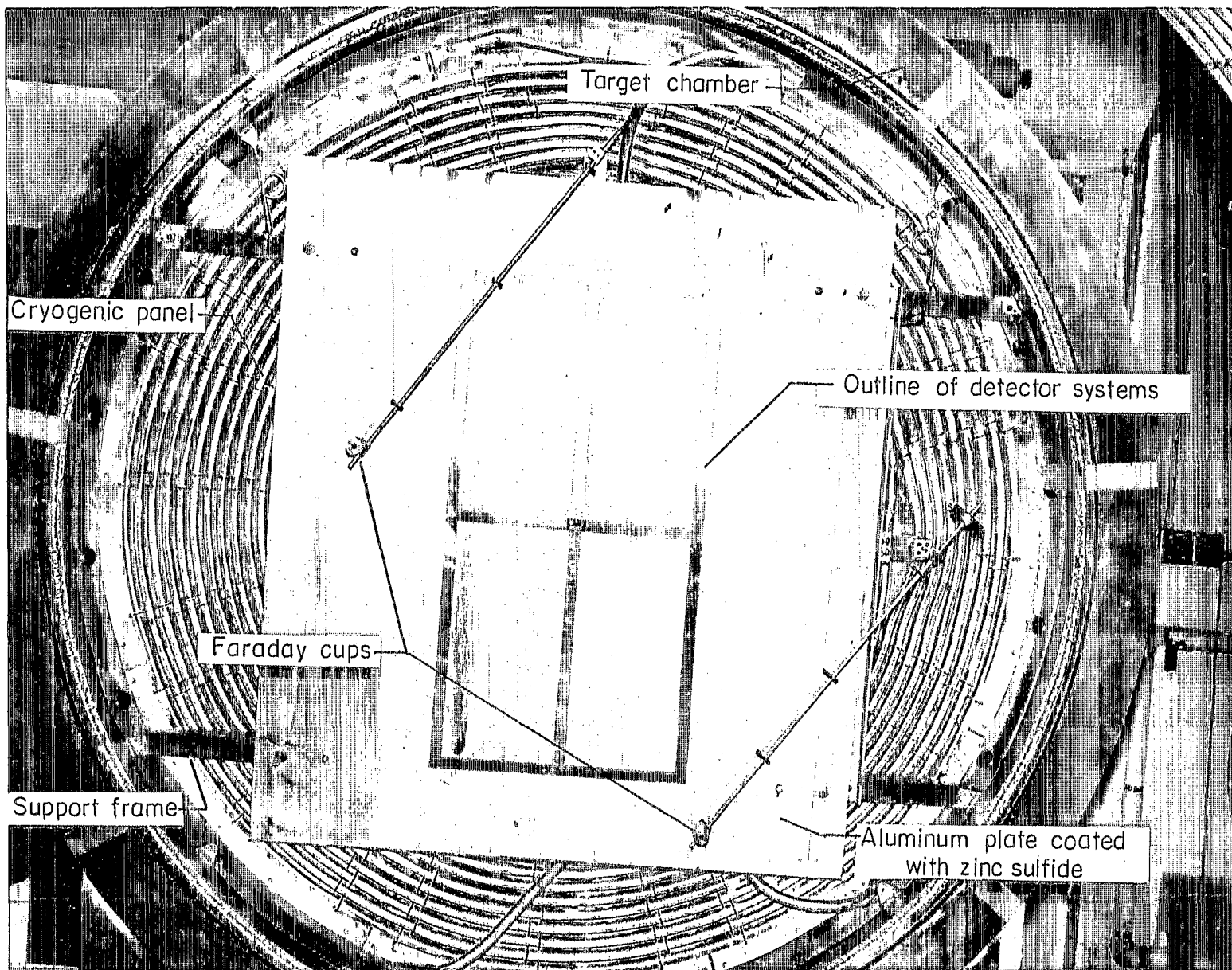
Figure 2.- Experimental setup used to determine the beam current uniformity.
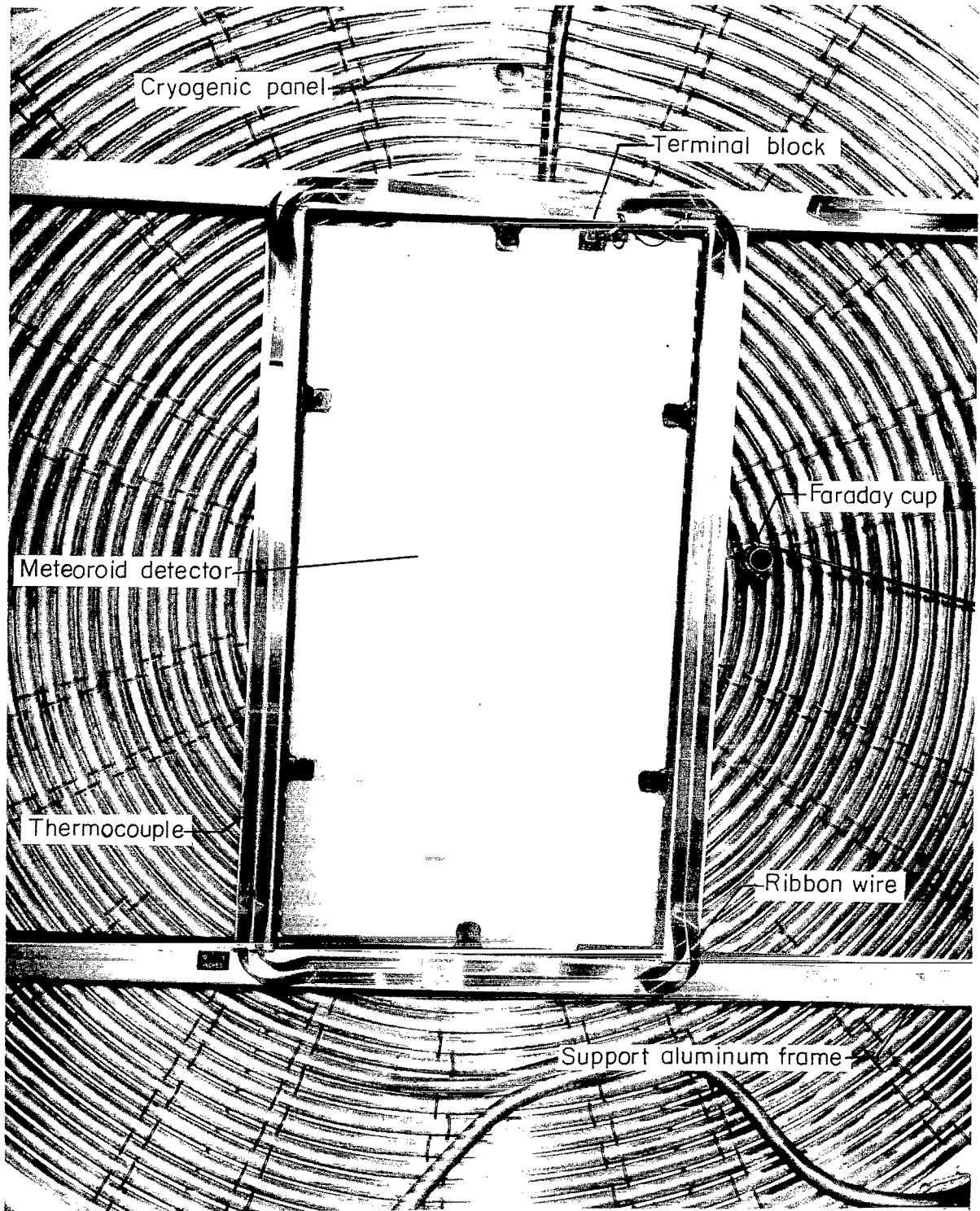
L-65-3435.1

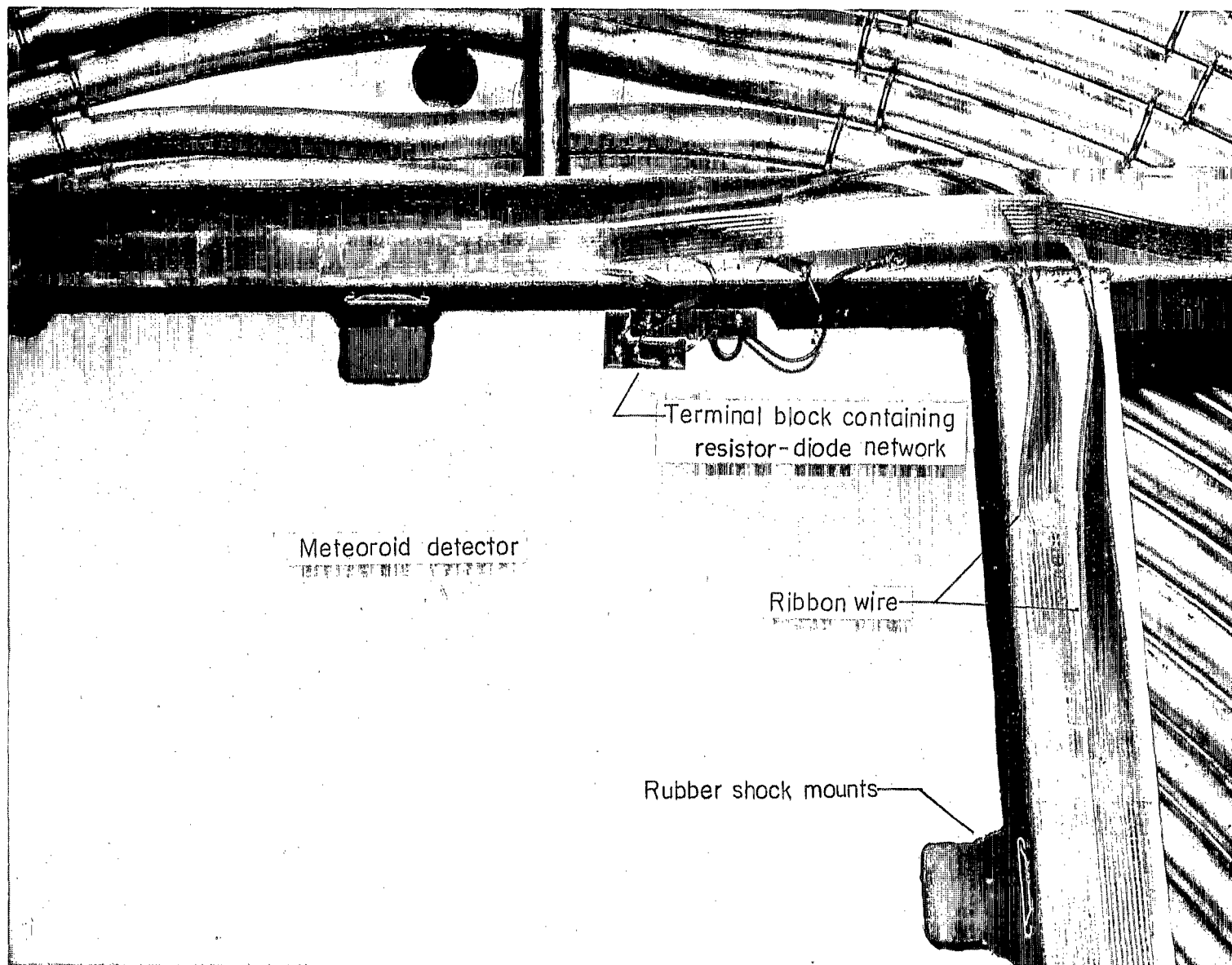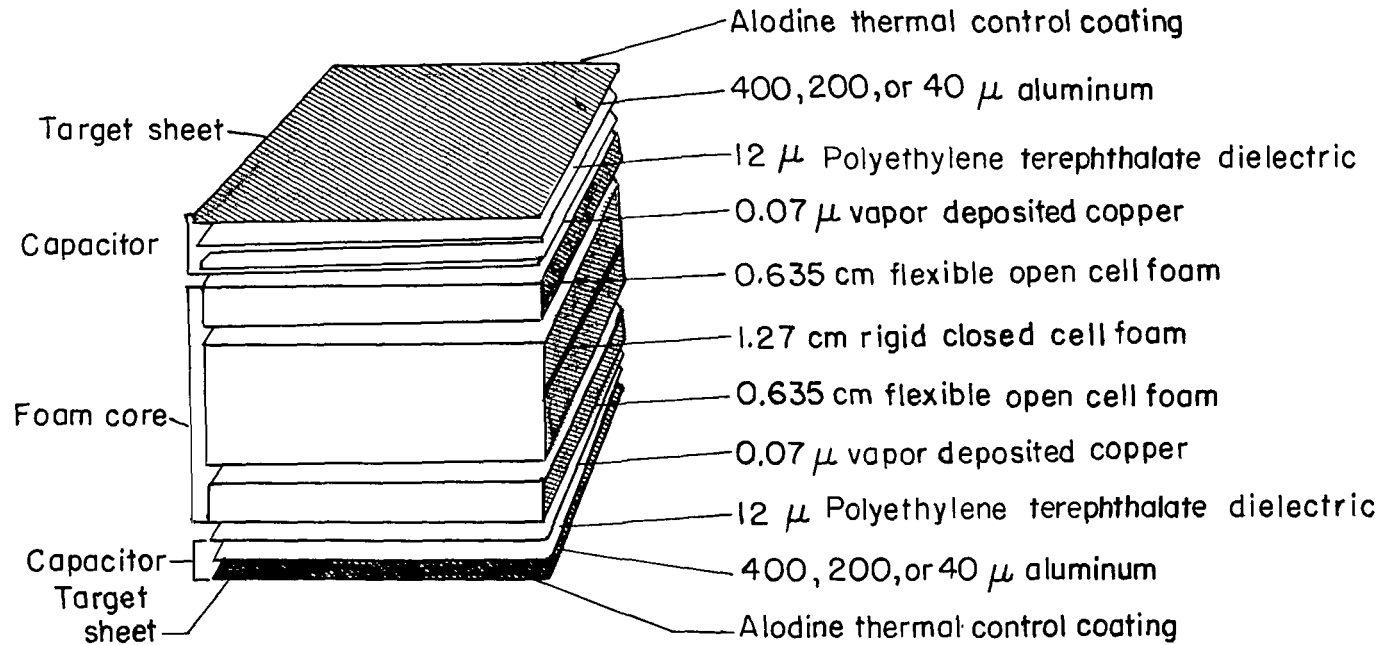Figure 3.- Experimental arrangement of detector system.

L-65-3409.1

18

Terminal block containing
resistor-diode network

Meteoroid detector

Ribbon wire

Rubber shock mounts

Figure 4.- Details of meteoroid detector system.

L-65-1656.1

Target sheet

Capacitor

Foam core

Capacitor

Target
sheet

Alodine thermal control coating

400,200,or 40 μ aluminum

12 μ Polyethylene terephthalate dielectric

0.07 μ vapor deposited copper

0.635 cm flexible open cell foam

1.27 cm rigid closed cell foam

0.635 cm flexible open cell foam

0.07 μ vapor deposited copper

12 μ Polyethylene terephthalate dielectric

400,200,or 40 μ aluminum

Alodine thermal control coating

Note : The 40 micron capacitors are bonded
directly to 2.54 cm rigid foam cores
with a 125 μ layer epoxy.

Figure 5.- Capacitor-type meteoroid penetration detector.
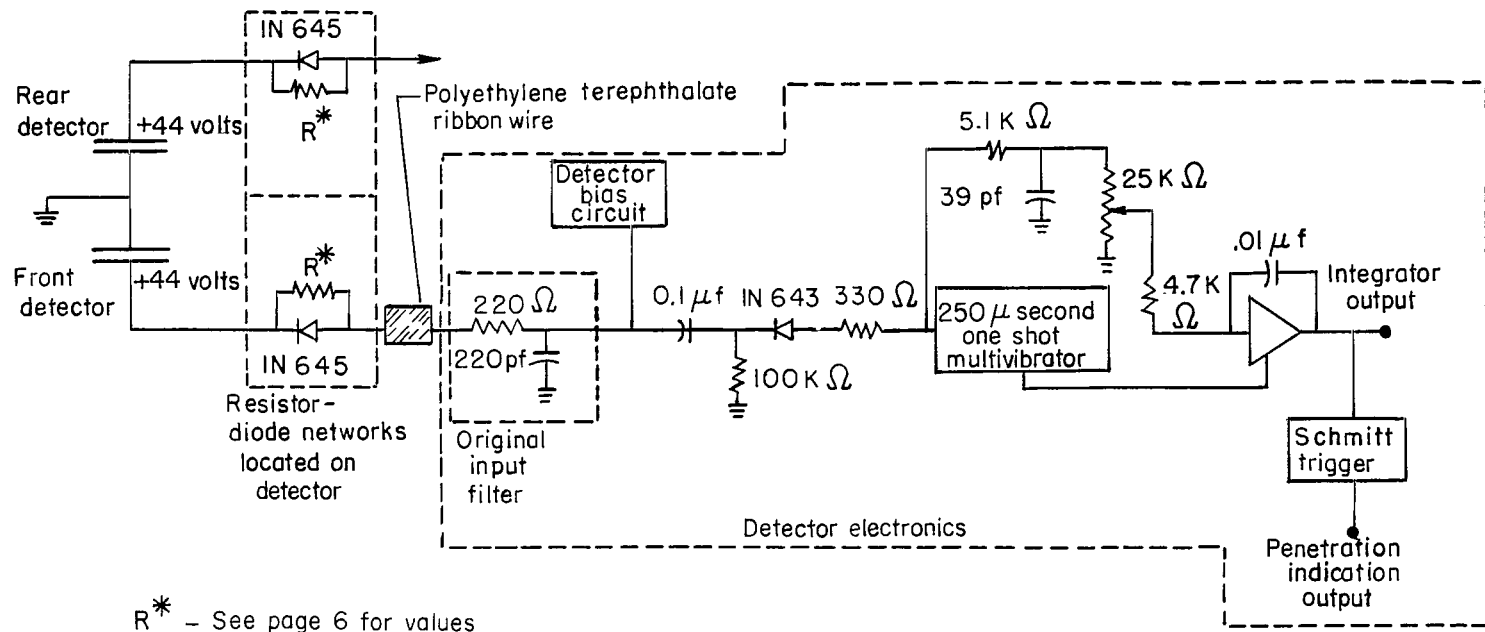
Figure 6.- Detector signal processing circuits.
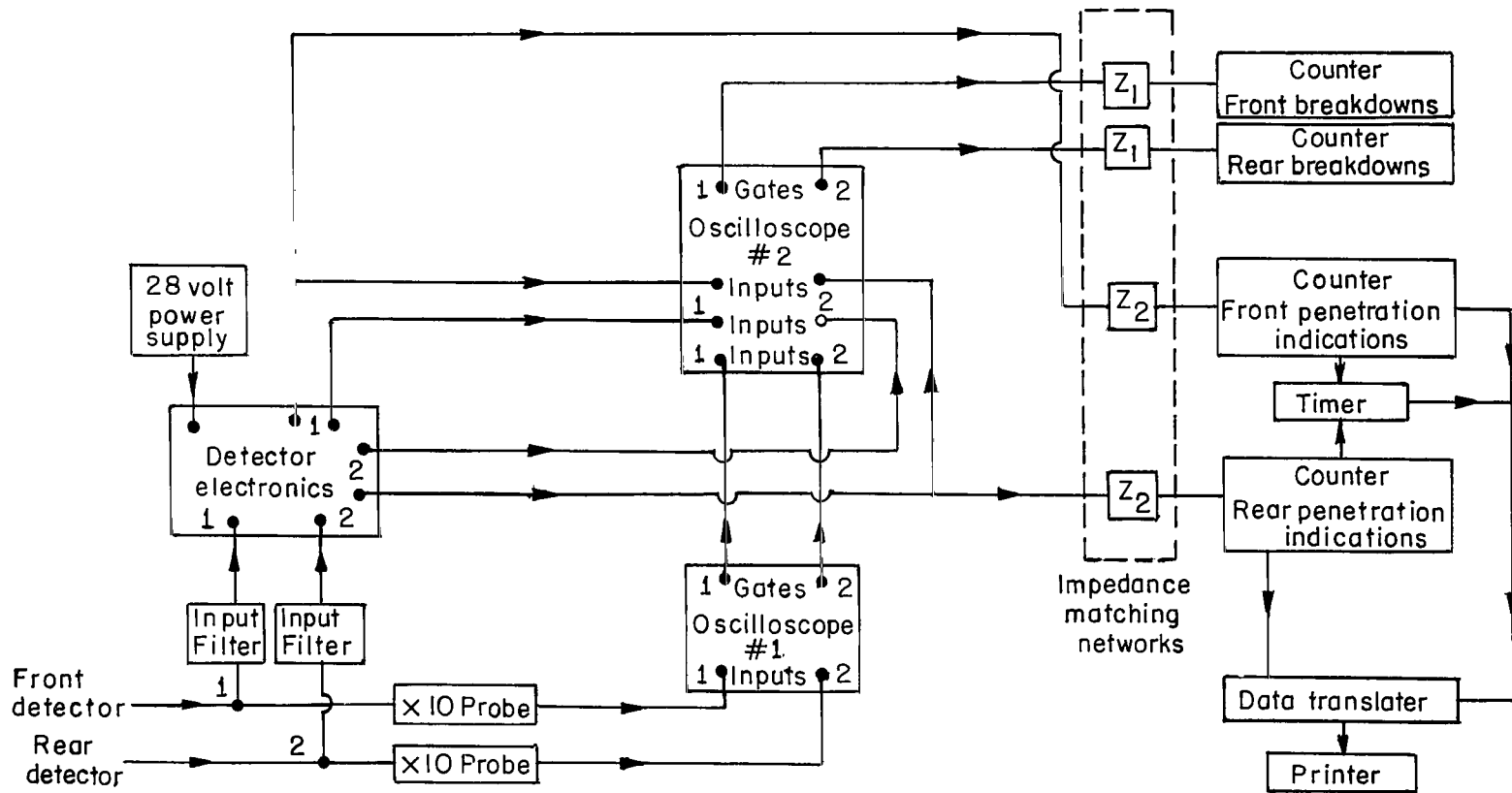
Figure 7.- Block diagram of signal processing and recording circuits.
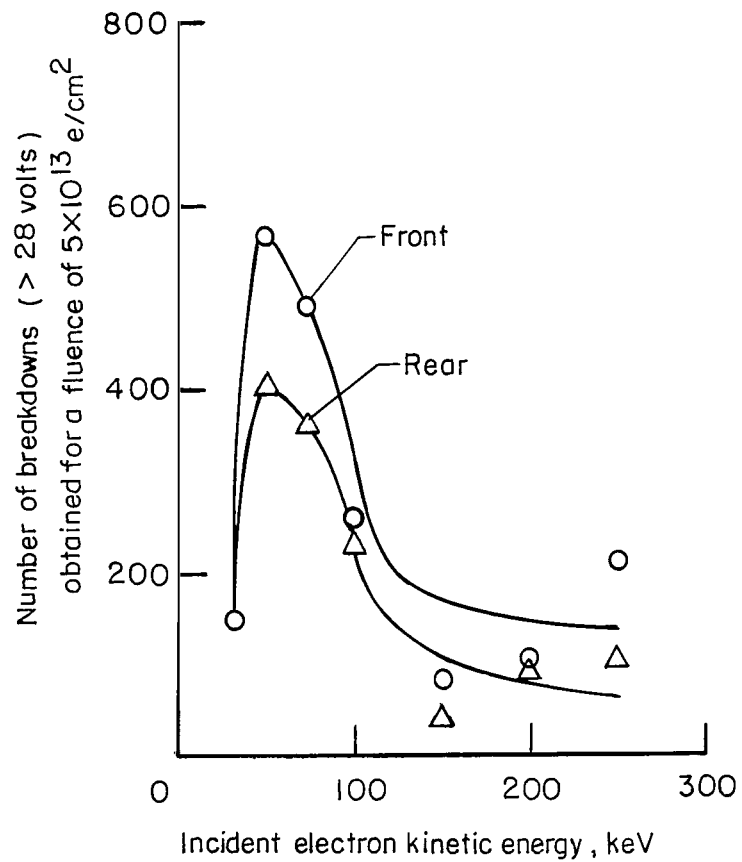
(a) Breakdowns.
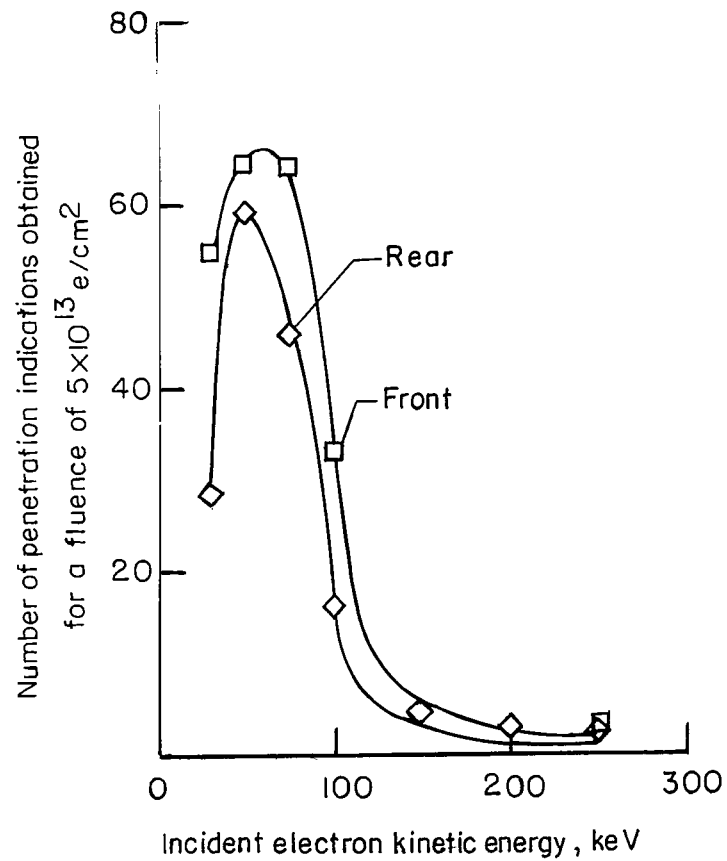
(b) Penetration indications.

Figure 8.- Dependence of number of breakdowns and penetration indications on kinetic energy at 197° K for detector system 2. Front detector is connected to channel 1 of readout electronics and rear detector is connected to channel 2.
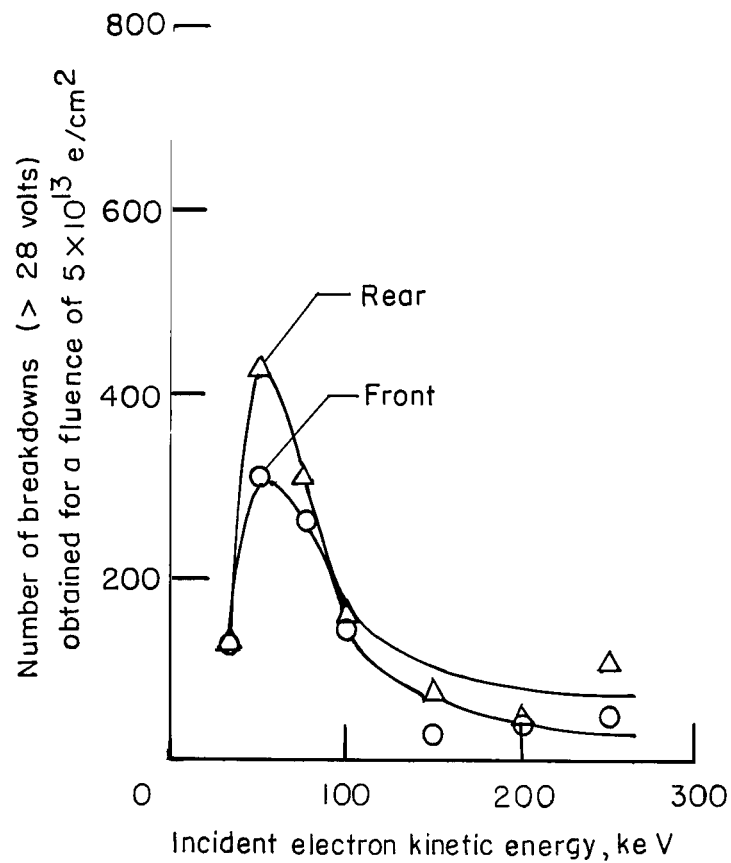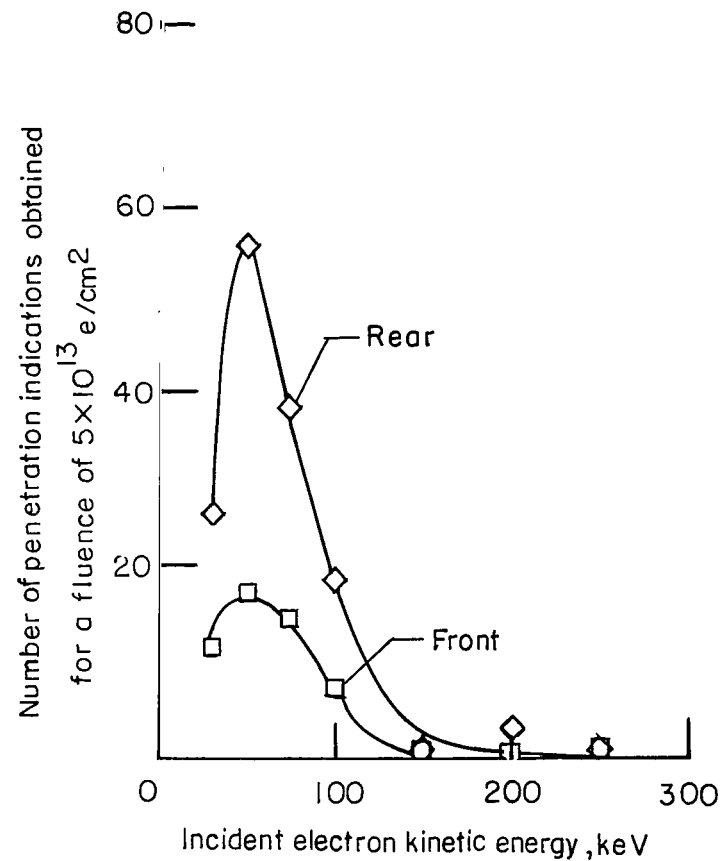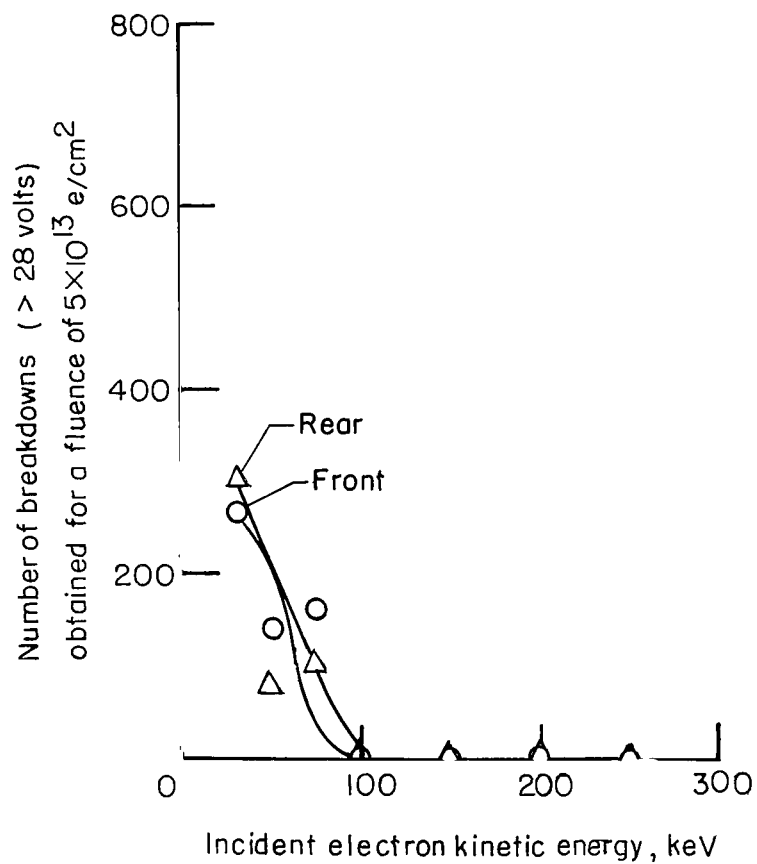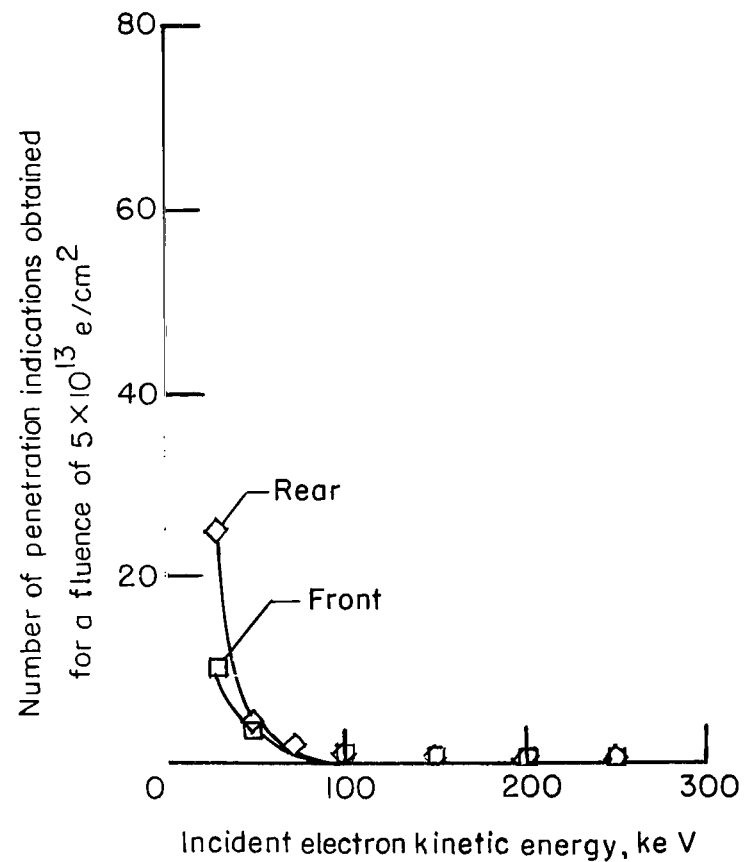
Number of breakdowns (> 28 volts)
obtained for a fluence of 5×10^{13} e/cm^2

800

600

400

Front

200

Rear

O   100   200   300

Incident electron kinetic energy, keV

(a) Breakdowns.

Number of penetration indications obtained
for a fluence of 5×10^{13} e/cm^2

80

60

40

Front

20

Rear

O   100   200   300

Incident electron kinetic energy, keV
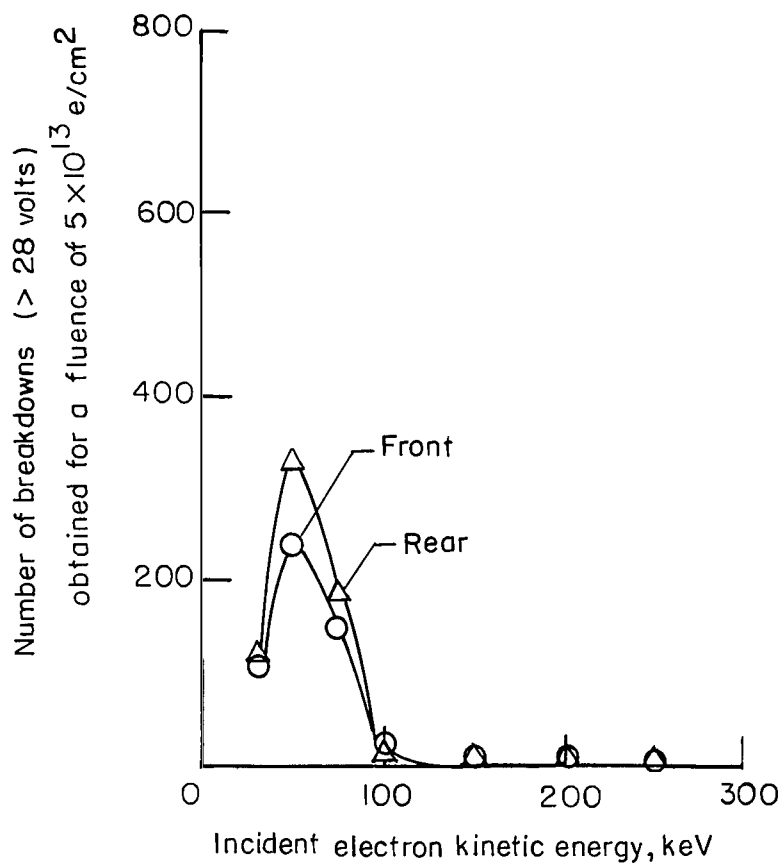
(b) Penetration indications.

Figure 9.- Dependence of number of breakdowns and penetration indications on kinetic energy at 297^0 K for detector system 2.
Front detector is connected to channel 1 of readout electronics and rear detector is connected to channel 2.
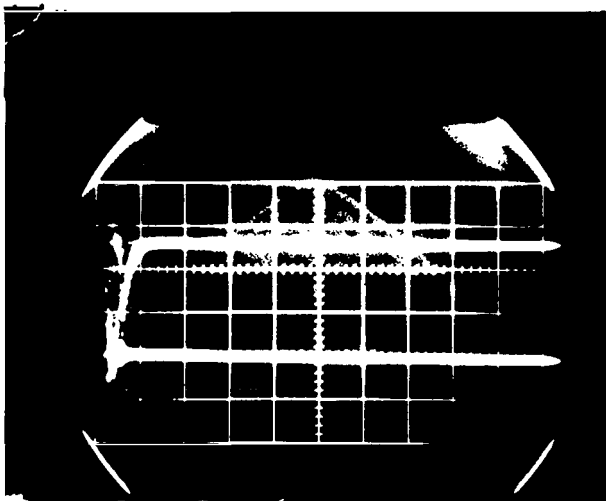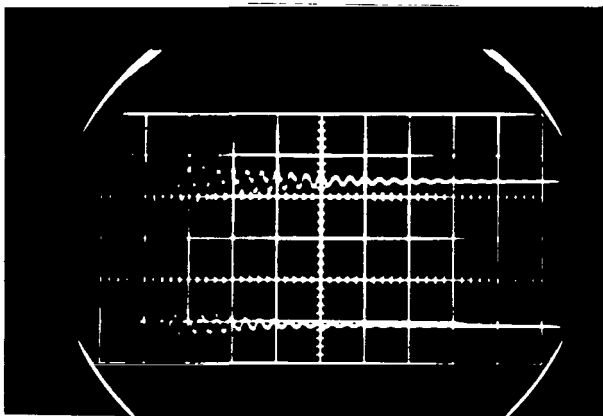
(a) Breakdowns.

(b) Penetration indications.

Figure 10.- Dependence of number of breakdowns and penetration indications on kinetic energy at 197° K for detector system 2. Front detector is connected to channel 2 of readout electronics and rear detector is connected to channel 1.

(a) Breakdowns.

(b) Penetration indications.

Figure 11.- Dependence of number of breakdowns and penetration indications on kinetic energy at 297° K for detector system 2.
Front detector is connected to channel 2 of readout electronics and rear detector is connected to channel 1.

Abscissa: $10\,\mu$ seconds/division
Ordinate : 20 volts/division
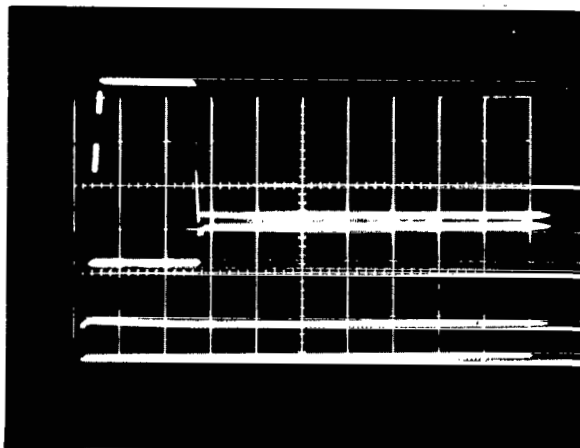
(1) Front breakdown

(2) Rear breakdown

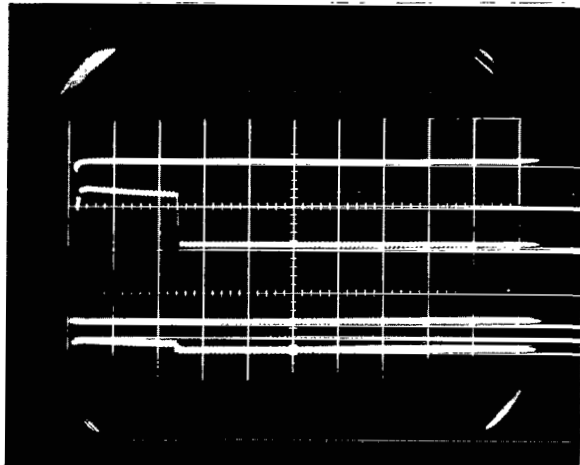Abscissa : $1\,\mu$ seconds/division
Ordinate : 50 volts/division

(1) Front breakdown

(2) Rear breakdown

Figure 12.- Photographs of breakdowns occurring in meteoroid detector system.

(1) Front integrator output
(2) Front penetration indication output

(3) Rear integrator output
(4) Rear penetration indication output

(1) Front penetration indication output

(2) Front integrator output

(3) Rear penetration indication output
(4) Rear integrator output

Abscissa: 100 μ seconds/division   Ordinate: 2 volts/division for integrator output
5 volts/division for penetration
indication output

Figure 13.- Photographs of integrator output and penetration indication output from meteoroid detector system.

"The aeronautical and space activities of the United States shall be conducted so as to contribute . . . to the expansion of human knowledge of phenomena in the atmosphere and space. The Administration shall provide for the widest practicable and appropriate dissemination of information concerning its activities and the results thereof."

— NATIONAL AERONAUTICS AND SPACE ACT OF 1958

NASA SCIENTIFIC AND TECHNICAL PUBLICATIONS

TECHNICAL REPORTS: Scientific and technical information considered important, complete, and a lasting contribution to existing knowledge.

TECHNICAL NOTES: Information less broad in scope but nevertheless of importance as a contribution to existing knowledge.

TECHNICAL MEMORANDUMS: Information receiving limited distribution because of preliminary data, security classification, or other reasons.

CONTRACTOR REPORTS: Scientific and technical information generated under a NASA contract or grant and considered an important contribution to existing knowledge.

TECHNICAL TRANSLATIONS: Information published in a foreign language considered to merit NASA distribution in English.

SPECIAL PUBLICATIONS: Information derived from or of value to NASA activities. Publications include conference proceedings, monographs, data compilations, handbooks, sourcebooks, and special bibliographies.

TECHNOLOGY UTILIZATION PUBLICATIONS: Information on technology used by NASA that may be of particular interest in commercial and other non-aerospace applications. Publications include Tech Briefs, Technology Utilization Reports and Notes, and Technology Surveys.

Details on the availability of these publications may be obtained from:

SCIENTIFIC AND TECHNICAL INFORMATION DIVISION

NATIONAL AERONAUTICS AND SPACE ADMINISTRATION
Washington, D.C. 20546